Long lifetime and efficient emission from Er3+ ions coupled to Si nanoclusters in Si-rich SiO2 layers

L. Khomenkova, F. Gourbilleau, J. Cardin, O. Jambois, B. Garrido, R. Rizk

Long lifetime and efficient emission from Er^{3+} ions coupled to Si nanoclusters in Si-rich SiO_2 layers

L. Khomenkova [a,*], F. Gourbilleau [a], J. Cardin [a], O. Jambois [b], B. Garrido [b], R. Rizk [a]

[a] CIMAP, UMR CEA/CNRS/ENSICAEN/University of CAEN, 6 Bd Maréchal Juin, 14050 Caen Cedex, France
[b] EME, Departament d'Electrònica, IN2UB, Universitat de Barcelona, Martí i Franquès 1, 08028 Barcelona, Spain

A B S T R A C T

Reactive magnetron co-sputtering of two confocal SiO_2 and Er_2O_3 cathodes in argon–hydrogen plasma was used to deposit Er-doped Si-rich SiO_2 layers. The effects of the deposition conditions (such as RF power applied on each cathode and total plasma pressure) and annealing treatment (temperature and duration) on structural, compositional and photoluminescence (PL) properties of the layers were examined. It was found that a significant enhancement of both Er^{3+} PL intensity and emission lifetime up to 9 ms have been reached through monitoring of the conditions of both deposition process and annealing treatment. The effective absorption cross section and the fraction of Er ions coupled to Si clusters were analyzed. It was shown an increase of the fraction of Er^{3+} ions coupled to Si up to 11%.

Keywords:
Si-rich silicon oxide
Erbium
Photoluminescence
Infrared absorption
Refractive index
Magnetron sputtering

1. Introduction

The transition in the internal 4f shell of the Er^{3+} ions results in an emission at 1.54 μm, which corresponds to the minimum of absorption of the silica-based optical fibers. Therefore, during the last decades a great attention was paid to the Er-doped SiO_2 materials developed for erbium-doped optical amplifiers and lasers.

In a laser gain medium, a long upper-state lifetime, τ, is necessary in order to reach a significant population inversion and to maintain a relatively low pump power. The gain efficiency of a laser also depends on the emission cross section, σ, (apart from other factors); the threshold pump power is inversely proportional to the product of upper-state lifetime and emission cross section (called the $\sigma-\tau$ product). Unfortunately, Er-doped-SiO_2 materials have a very low absorption cross section of Er^{3+} ions, $\sigma\sim10^{-21}$ m^2 [1–3] that requests large pump powers from expensive lasers for optical amplification. On the other hand, numerous Er-doped Si-based materials have specific drawbacks, for example, Auger de-excitation or energy back-transfer processes [2].

Recently an enhancement of about two orders of magnitude of Er^{3+} photoluminescence (PL) has been demonstrated for Er-doped Si-rich SiO_2 (Er-SRSO) in comparison with Er-doped SiO_2 [4–9]. This effect was attributed to the sensitizing role of Si nanoclusters (Si-nc) towards the neighbouring Er^{3+} ions [10] that leads to an increase of the effective absorption cross section σ_{eff} up to about 10^{-16} cm^{-2} [11]. Either crystalline and/or amorphous Si-ncs are efficient sensitizers of Er^{3+} ions [12,13]. The optimal size of Si-nc and the critical distance of Si-nc/Er interaction were found to be 3–4 nm [14] and 0.5 nm [15,16], respectively. Nevertheless, the question concerning the number of optically active Er^{3+} ions and their fraction coupled to Si-nc is still open, although recent studies reported, however, that only few percent of the total amount of Er ions were coupled to Si-nc [8,17].

The efficiency of the indirect excitation of Er^{3+} ions (via Si-nc) is affected by the density, size and distribution of Si-nc, as well as by the concentration and chemical environment of the Er^{3+} ions. All these factors are strongly dependent on the deposition conditions and post-deposition annealing treatment [14,16–18]. Therefore, their monitoring results in the production of Er-SRSO materials enabling the achievement of an optical gain that should offer the possibility to create low-cost compact amplifier and laser compatible with the CMOS technology.

In this paper, a novel approach for our team is explored to increase the Si-nc/Er coupling rate. It consists in the reactive co-sputtering of two separate Er_2O_3 and SiO_2 cathodes, instead of the reactive sputtering of a unique SiO_2 cathode topped by Er_2O_3 chips described in Ref. [18]. The effects of the deposition conditions and annealing treatment have been studied with the aim of optimizing the Er-SRSO layers in terms of high PL emission and long lifetime at 1.54 μm.

* Corresponding author. Tel.: +33 231 45 26 56.
E-mail address: larysa.khomenkova@ensicaen.fr (L. Khomenkova).

2. Experimental

The layers investigated have been fabricated by reactive RF magnetron co-sputtering of 2 in confocal pure SiO_2 and Er_2O_3 targets under argon–hydrogen mixture onto 2–4 in p-type silicon substrates. The incorporation of Si in the sub-stoichiometric layers was due to the reactive ability of hydrogen to reduce the oxygen species in the plasma. This results in the control of Si excess in the layers through the variation of hydrogen rate r_H [19]. This latter is considered as $r_H = F_{H_2}/(F_{H_2} + F_{Ar})$, where F_{H_2} and F_{Ar} are the values of the hydrogen and argon flow, respectively. The total flow of both gases was kept constant at 10 sccm, while the variation of F_{H_2} from 2 to 8 sccm corresponds to a change of r_H value in the range 20–80%. Moreover, the substrate temperature, T_S, allows also some change of the amount of Si excess incorporated in the layers [20,21].

In the present study, the effects of the RF power applied on each cathode (called hereafter $RFP_{Er_2O_3}$ and RFP_{SiO_2}), the total plasma pressure, P_{total}, annealing time, t_A, and temperature, T_A, were investigated for the layers deposited at $r_H = 50\%$ and $T_S = 100\,^{\circ}C$. The annealing was performed in nitrogen flow at T_A varied between 550 and 1100 °C and t_A ranging between 2 and 60 min.

The SIMS and XPS methods were used to determine the concentration of Er and amount of Si excess which was estimated with respect to pure SiO_2.The microstructure of the as-deposited and annealed layers were studied also by means of Fourier transform infrared (FTIR) spectroscopy. The spectra were recorded under normal and Brewster (65°) incidences in the range 500–4000 cm^{-1} with a Nicolet Nexus spectrometer. The Si excess was also estimated considering the difference between the TO_3 peak positions observed for as-deposited layers and a pure sputtered SiO_2. The thickness and the refractive index of the layers were controlled by spectroscopic ellipsometry and/or M-lines measurements [22,23]. The M-lines measurement was performed by means of a He–Ne laser emitting at 632.8 nm polarized in transverse electric mode.

The light emission properties of the films have been investigated by means of PL measurements. The PL spectra were recorded using a Jobin Yvon 1 m single grating monochromator and with a North coast Ge-detector cooled with liquid nitrogen. The excitation source was Ar^+-laser operating at 476.5 nm to ensure that Er^{3+} emission was only stimulated by the energy transfer from the Si sensitizers. The pumping photon flux was in the range 1×10^{16}–4×10^{20} ph/cm^2 s. The PL signal was recorded through a SRS lock-in amplifier (SP830 DPS) referenced to the chopping frequency of light of 20 Hz. To compare different samples, all PL spectra were normalized on the value of the excited volume. The time-resolved Er^{3+} PL was measured with the PL setup mentioned above, the signal being displayed by a Tektronix oscilloscope (TDS 3012B). All the measurements were performed at room temperature and corrected on the setup response.

3. Results and discussion

3.1. The effect of total plasma pressure

The effect of the total plasma pressure, P_{total}, was studied for the layers deposited at 1–4 mTorr. It was observed that an increase of P_{total} from 1 to 4 mTorr results in a decrease of the refractive index from 1.53 to 1.48 for as-deposited layers (Fig. 1a, curve 1). Such behaviour of the refractive index could be explained by a decrease of the Si excess in the samples when the plasma pressure increases. Their annealing at high temperature leads to the increase of the refractive index (Fig. 1a, curve 2), owing to the expected improvement of samples' compactness, while keeping the same evolution with respect to the plasma pressure.

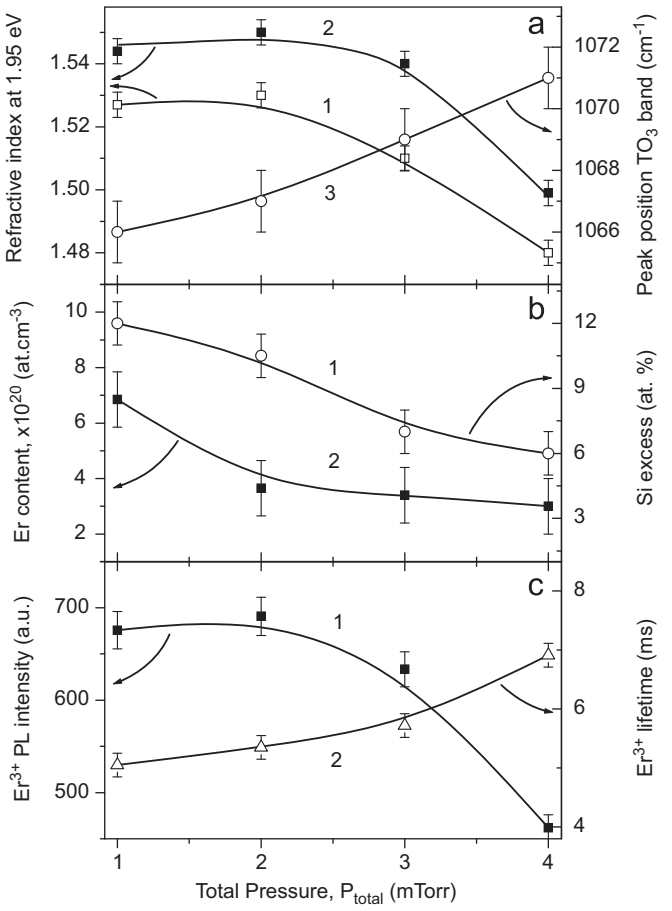

Fig. 1. (a) Variation of the refractive index (at 632.8 nm) of as-deposited (1) and annealed at 900 °C during 60 min (2) layers against P_{total}. Curve 3 shows the variation of peak position of TO_3 vibration band in as-deposited layers with P_{total}. (b) Variation of the Si excess (1) as estimated from evolution of FTIR spectra measured at the normal incidence. Curve 2 represents the Er content in the layers versus P_{total} obtained by SIMS method. (c) Effect of P_{total} on the Er^{3+} PL intensity at 1.53 μm (1) and lifetime (2) obtained for the layers annealed at 900 C during 60 min. The Er^{3+} PL was recorded under non-resonant excitation (476.5 nm and a photon flux of 4×10^{19} ph/cm^2 s).

The decrease of Si excess with P_{total} was confirmed by the evolution of the FTIR spectra recorded under normal incidence of the light. As one can see, the peak position of TO_3 vibration band shows a gradual shift from 1066 to 1071 cm^{-1} when P_{total} increases (Fig. 1a, curve 3). Using the method described in Ref. [24], the Si excess estimated from FTIR data was found to decrease from 12 to 6 at% (Fig. 1b, curve 1). The latter was also confirmed by XPS measurements reporting a decrease of the Si excess from 11 at% to 5% (not shown).

On the other hand, Er content was found to increase from 3.4×10^{20} to 6.8×10^{20} at/cm^3 when P_{total} decreases from 4 to 1 mTorr. This indicates that the decrease of P_{total} favours the incorporation of Si excess and Er ions in the layers.

The variation of PL parameters with P_{total} is presented in Fig. 1c. As one can notice, the P_{total} increase favours longer Er^{3+} lifetime, but lower PL intensity. This could be explained by the variation of both Si excess and Er content in the layers. The increase of the Si excess allows the increase of the number of Er ions benefiting from the sensitizing effect of Si-nc, which consequently leads to the increase of the PL intensity. However, the increase of Er

content may result in the occurrence of up-conversion phenomena and concentration quenching processes. Since the higher intensity is observed for the layers deposited at $P_{total} = 1–3$ mTorr, while the longer lifetime is obtained for $P_{total} = 3–4$ mTorr, the effect of the other deposition conditions and annealing treatment will be investigated for the layers deposited with $P_{total} = 3$ mTorr.

3.2. The effect of the power applied on cathodes

The increase of the power applied on the SiO_2 cathode at constant $RFP_{Er_2O_3}$, T_s and r_H leads to the decrease of the Si excess (not shown). This demonstrates that the Si excess in the layer can be also monitored by RFP_{SiO_2} in addition to r_H, as evidenced elsewhere [19–21]. This is corroborated by the evolution of FTIR spectra and of refractive index with RFP_{SiO_2}. For example, for the layers deposited with $P_{total} = 3$ mTorr, the decrease of the refractive index from 1.54 to 1.50 was observed when RFP_{SiO_2} increases from 90 to 180 W, while the corresponding FTIR spectra show a shift of TO_3 peak position towards the high-frequency side. Besides, the simultaneous increase of the contribution of the TO_4–LO_4 doublet reflects the increase of the disorder within the host oxide (not shown).

On the other hand, the increase of $RFP_{Er_2O_3}$ value from 9 to 18 W at constant RFP_{SiO_2} does not affect practically the refractive index and FTIR spectra, i.e. the amount of the Si excess incorporated in the layers.

The dependence of the Er^{3+} PL properties on RFP_{SiO_2} and $RFP_{Er_2O_3}$ is more complex. The increase of RFP_{SiO_2} from 30 to 60 W – all other parameters being fixed – leads to the increase of Er^{3+} PL intensity and the decrease of Er^{3+} lifetime. At the same time, the increase of $RFP_{Er_2O_3}$ from 9 to 18 W results in the enhancement of Er^{3+} emission, whereas further increase up to 30 W favours the PL quenching and therefore the up-conversion process [21]. This is confirmed by the decrease of the Er^{3+} lifetime that could be connected with the up-conversion process occurring in samples with relatively high Er concentration. The analysis of the obtained results allows one to conclude that the ratio $RFP_{SiO_2}/RFP_{Er_2O_3} = 9–10$ is found to be optimal to reach high-efficient PL and lifetime (more than 4.5 ms).

3.3. Effect of annealing treatment on the properties of Er-SRSO layers

It is known that the annealing of sub-stoichiometric SiO_x layers at high temperature induces a phase separation into Si and SiO_2 phases. This is illustrated by the variation of the refractive index as well as by the shifts of peak positions of TO_3 and LO_3 vibration bands (Fig. 2, curves 1 and 2) towards the position of their counterparts corresponding to pure SiO_2. It is worth to note that the formation of Si crystallites is accompanied by the preferable increase of LO_3 vibration band with respect to TO_3 band that is the signature of the formation of Si/SiO_2 interface and thus of Si nanoclusters.

The annealing of Er-SRSO layers at $T_A = 800–900$ °C during only 2 min results in a noticeable shift of peak position of either TO_3 or LO_3 vibration bands (Fig. 2). This shows evidence of fast demixing of SiO_x. Simultaneously, a sharp increase of the ratio of the intensities of LO_3 and TO_3 vibration bands was observed, which reaches a saturation regime for the long-time treatment (Fig. 2, curve 3). Such a behaviour is indicative of the formation of the Si clusters during the first few minutes, while the long-time annealing leads mainly to the improvement of the matrix as reflected by the decreasing contribution of TO_4–LO_4 doublet [21].

These observations are corroborated by the appearance of an intense Er^{3+} emission after short-time annealing although the corresponding lifetime is still low, about 2 ms (Fig. 3). The longer

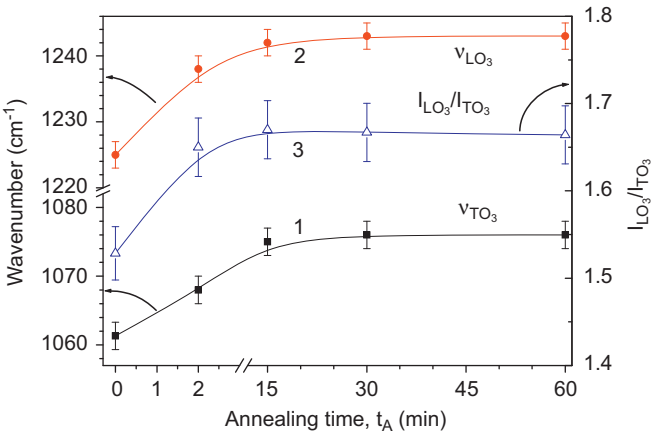

Fig. 2. Evolution of the peak position of TO_3 (1) and LO_3 (2) vibration bands in function of the annealing duration. Curve 3 presents the variation of the ratio of the intensity of LO_3 band and TO_3 band with annealing duration. The data were taken from FTIR spectra measured under Brewster angle incidence. The annealing temperature was 800 °C.

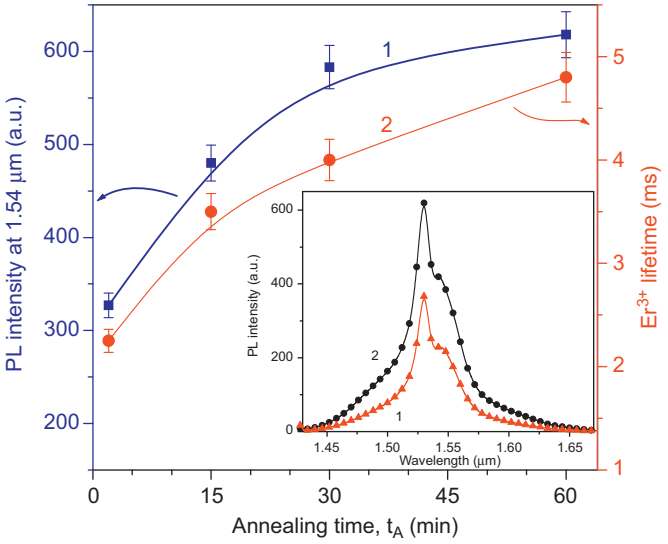

Fig. 3. Er^{3+} PL intensity at 1.53 μm (1) and corresponding lifetime (2) versus annealing time for two pumping photon flux, respectively, 2×10^{19} and 4×10^{16} ph/cm^2 s. The insert compares the PL spectra of two couple of values of the power applied on cathodes, $RFP_{SiO_2} = 150$ W and $RFP_{Er_2O_3} = 15$ W (curve 1) and $RFP_{SiO_2} = 180$ W and $RFP_{Er_2O_3} = 21$ W (curve 2). The samples were annealed during 60 min. The same annealing temperature of 800 °C and excitation wavelength of 476 nm were used for all studied layers.

annealing leads to a significant increase of both Er^{3+} PL intensity and lifetime (from 2.3 up to 6 ms).

The annealing of the layers at moderate temperature (550–600 °C) during 60 min leads also to the appearance of Er^{3+} emission with lifetime of about 2 ms (Fig. 4). It is obvious that at such temperature, crystalline Si clusters could not be formed. In this case, the excitation of Er ions occurs through very small Si clusters, such as the small agglomeration of Si atoms. It is possible that the increase of the annealing temperature results in the increase of Si-nc average sizes, but even at 900 °C they are still amorphous and are not easy to observe by transmission electron microscopy [21].

The increase of annealing temperature from 550 to 900 °C results in the gradual increase of Er^{3+} lifetime from 2.3 to 9 ms, while the PL intensity, at first, increases until a maximum at 700–750 °C and then gradually decreases (Fig. 4).

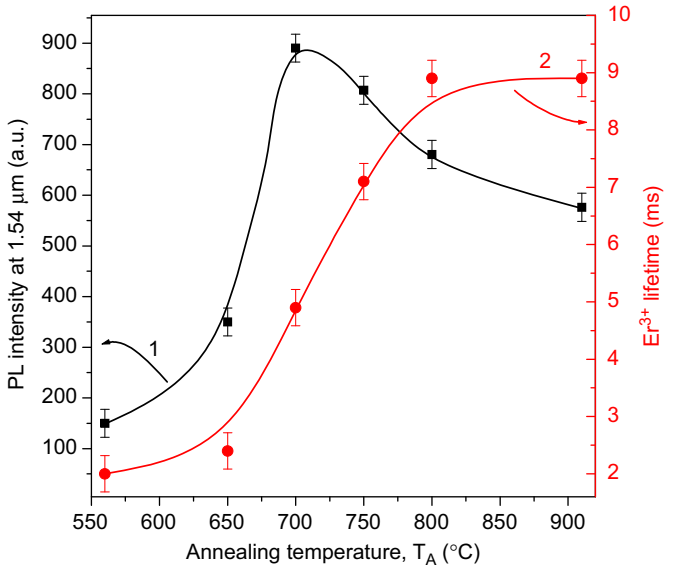

Fig. 4. Dependence of the Er PL intensity at 1.53 µm (1) and lifetime (2) on the annealing temperature obtained with non-resonant excitation and photon flux of 2×10^{19} ph/cm^2 s for curve 1 and 4×10^{16} ph/cm^2 s for curve 2.

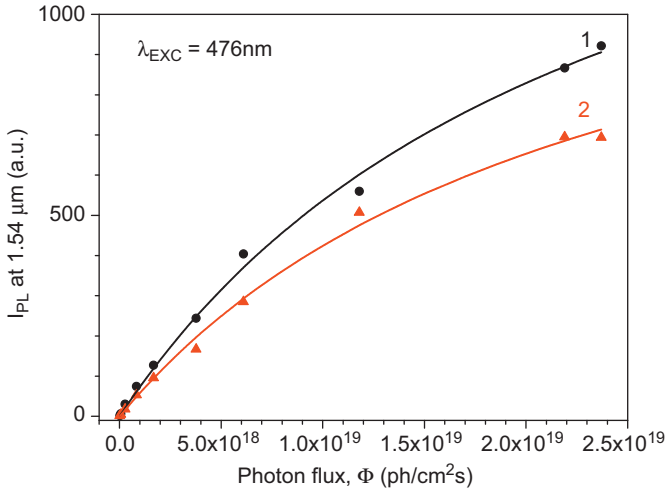

Fig. 5. The dependence of Er^{3+} PL intensity at 1.53 µm for the layers deposited at $P_{total} = 2$ and 3 mTorr and annealed at 900 °C during 60 min.

It is worth to note that the highest intensity of Er^{3+} emission in the present study was observed for the layers deposited at $RFP_{SiO_2} = 180$ W and $RFP_{Er_2O_3} = 21$ W (inset of Fig. 3, curve 2). The lifetime in this case was about 6 ms. On the other hand, the layers showing a lifetime as high as 9 ms, were prepared with $RFP_{SiO_2} = 150$ W and $RFP_{Er_2O_3} = 15$ W. The corresponding PL intensity was still high (inset of Fig. 3, curve 1).

3.4. Dependence of the PL properties on pumped photon flux

The dependence of Er^{3+} PL intensity on the photon flux was obtained under 476.5 nm excitation to study the coupling between Si clusters and Er^{3+} ions. The results are presented in Fig. 5 for layers deposited under a plasma pressure of 2 and 3 mTorr and annealed at 900 °C during 60 min.

From rate equations [25] and assuming as negligible de-excitation processes such as up-conversion, etc. are negligible, the intensity of the steady-state PL could be described by the formula

$$I_{PL}^{Er} = KSd \frac{\sigma_{eff}\tau_{PL}\varphi N_{Er}}{\tau_{RAD}(1 + \sigma_{eff}\tau_{PL}\varphi)} \quad (1)$$

where S is the excited surface, d is the sample thickness, σ_{eff} is the effective absorption cross section of Er, τ_{PL} and τ_{RAD} are the measured and radiative lifetime, φ is the photon flux, N_{Er} is the total Er content in the layer, K is the measurement constant corresponding to our setup.

The fitting of the experimental data presented in Fig. 5 was performed using formula (1). The σ_{eff} was found to be $\sim 1 \times 10^{-17}$ cm^2. On the other hand, the time-resolved PL measurements performed with non-resonant excitation line for different values of photon flux allows also an estimate of σ_{eff}, as described in Ref. [18]. According to the method developed in Ref. [18], the σ_{eff} was estimated from the linear part of the dependence of $(1/\tau_{rise} - 1/\tau_{PL})$ versus φ observed for lower photon fluxes and the obtained value for σ_{eff} (1.2×10^{-17} cm^2) was found very close to that reported above.

The comparison of the efficiency of Er^{3+} emission from the layers studied in this paper with their best counterparts from Ref. [18] measured with the same conditions shows that the first ones are four times more efficient than the last ones. Based on this result, a rough estimation of the fraction of Er ions coupled to Si-nc was performed. The layers deposited with $P_{total} = 3$ mTorr contain less Si excess (5 at% instead of 7 at% observed in Ref. [18]), while those prepared at 2 mTorr contains about 10 at%. Taking into account that both layers have the same Er content and considering the difference in Si excess, we can consider that such an efficiency of Er^{3+} emission could originate from the higher coupling rate between Si-nc and Er^{3+} ions. Besides, the better environment of Er ions is confirmed by the higher lifetime and could be also responsible for the increase of the PL intensity. Finally, the fraction of Er^{3+} ions coupled to Si clusters was found about 11% of the total concentration of the Er ions in layers instead of 3% reported in Ref. [18]. In spite of these promising results further improvements are required to reach a net gain in such Er-SRSO layers.

4. Conclusions

Reactive magnetron sputtering from two confocal SiO_2 and Er_2O_3 cathodes in argon–hydrogen plasma was used to deposit Er^{3+}-doped Si-rich SiO_2 layers. It was observed that the variation of RF power applied on each cathode and total plasma pressure, followed by an appropriate annealing treatment, allows the control of both Er^{3+} PL intensity and lifetime. Optimum fabrication conditions were found to increase significantly the Er^{3+} emission and the lifetime from 4.5 to about 9 ms. The observation of comparable Er^{3+} PL intensities under resonant and non-resonant excitations is indicative of the efficient sensitizing role of Si clusters towards the coupled Er ions, while the high lifetime would reflect the quality of both host matrix and surrounding of the Er ions. The fraction of Er^{3+} ions coupled to Si clusters was found about 11% of the total Er concentration instead of 3% demonstrated earlier. Further improvements are still, however, needed to obtain a net gain in the Er-coupled Si nanocluster material.

Acknowledgements

We thank Prof. Christian Dufour from NIMPH team of CIMAP laboratory for fruitful discussions. This work is supported by the European Community through the LANCER Project (FP6-IST 033574).

References

[1] A. Polman, J. Appl. Phys. 82 (1997) 1.
[2] F. Priolo, G. Franzò, S. Coffa, A. Carnera, Phys. Rev. B 57 (1998) 4443.
[3] W. Miniscalco, in: M. Digonnet (Ed.), Rare-Earth-Doped Fiber Lasers and Amplifiers, Dekker, New York, 2001, p. 62.
[4] A.J. Kenyon, P.F. Trwoga, M. Federighi, C.W. Pitt, J. Phys.: Condens. Matter 6 (1994) L319.
[5] M. Fujii, M. Yoshida, Y. Kansawa, S. Hayaski, K. Yamamoto, Appl. Phys. Lett. 71 (1997) 1198.
[6] J.H. Shin, K. Kim, S. Seo, C. Lee, Appl. Phys. Lett. 72 (1998) 1092.
[7] G. Franzò, V. Vinciguerra, F. Priolo, Appl. Phys. A: Mater. Sci. Process 69 (1999) 3.
[8] M. Wodjak, M. Klik, M. Forcales, O.B. Gusev, T. Gregorkiewicz, L. Pacifici, G. Franzò, F. Priolo, F. Iacona, Phys. Rev. B 69 (2004) 233315.
[9] F. Gourbilleau, C. Dufour, M. Levalois, J. Vicens, R. Rizk, C. Sada, F. Enrichi, G. Battaglin, J. Appl. Phys. 94 (2003) 3869.
[10] K. Watanabe, M. Fujii, S. Hayashi, J. Appl. Phys. 90 (2001) 4761.
[11] F. Priolo, G. Franzò, D. Pacifici, V. Vinciguerra, F. Iacona, A. Irrera, J. Appl. Phys. 89 (2001) 264.
[12] D. Kovalev, J. Diener, H. Heckler, G. Polisski, N. Künzner, F. Koch, Phys. Rev. B. 61 (2000) 4485.
[13] G. Franzò, S. Boninelli, D. Pacifici, F. Priolo, F. Iacona, C. Bongiorno, Appl. Phys. Lett. 82 (2003) 3871.
[14] F. Gourbilleau, L. Levalois, C. Dufour, J. Vicens, R. Rizk, J. Appl. Phys. 95 (2004) 3717.
[15] J.H. Jhe, J.H. Shin, K.J. Kim, D.W. Moon, Appl. Phys. Lett. 82 (2003) 4489.
[16] F. Gourbilleau, C. Dufour, R. Madelon, R. Rizk, J. Lumin. 126 (2007) 581.
[17] B. Garrido, C. Garcia, P. Pellegrino, D. Navarro-Urrios, N. Daldosso, L. Pavesi, F. Gourbileau, R. Rizk, Appl. Phys. Lett. 89 (2006) 163103.
[18] B. Garrido, C. García, S.-Y. Seo, P. Pellegrino, D. Navarro-Urrios, N. Daldosso, L. Pavesi, F. Gourbilleau, R. Rizk, Phys. Rev. B. 76 (2007) 245308.
[19] C. Ternon, F. Gourbilleau, X. Portier, P. Voivenel, C. Dufour, Thin Solid Films 419 (2002) 5.
[20] L. Khomenkova, F.Gourbilleau, J. Cardin, R. Rizk, Physica E 2008, in press, doi:10.1016/j.physe.2008.08.016.
[21] F. Gourbilleau, L. Khomenkova, D. Bréard, C. Dufour, R. Rizk, Physica E 2008, in press, doi:10.1016/j.physe.2008.08.057.
[22] R.M.A. Azzam, N.M. Bashara, Ellipsometry and Polarized Light, North-Holland, Amsterdam, 1977.
[23] T. Schneider, D. Leduc, C. Lupi, J. Cardin, H. Gundel, C. Boisrobert, J. Appl. Phys. 103 (2008) 063110.
[24] N. Tomozeiu, Appl. Surf. Sci. 25 (2006) 376.
[25] R. Paschotta, P.R. Barber, A.C. Tropper, D.C. Hanna, J. Opt. Soc. Am. B 14 (1997) 1213.